Remote Sensing of Environment 126 (2012) 160–173

Contents lists available at SciVerse ScienceDirect

Remote Sensing of Environment

journal homepage: www.elsevier.com/locate/rse

Prediction of soil properties using a process-based forest growth model to match satellite-derived estimates of leaf area index

Nicholas C. Coops [a,*], Richard H. Waring [b], Thomas Hilker [b]

[a] Department of Forest Resource Management, 2424 Main Mall, University of British Columbia, Vancouver, Canada V6T 1Z4
[b] College of Forestry, Oregon State University, Corvallis, OR, 97331, United States

ARTICLE INFO

Article history:
Received 20 May 2012
Received in revised form 15 August 2012
Accepted 19 August 2012
Available online xxxx

Keywords:
Ecoregions
Soil water holding capacity
Fertility index
MODIS leaf area index
Climate-driven models
Remote sensing
3-PG forest growth model

ABSTRACT

Without better estimates of soil properties than are currently available from coarse-scale maps, it is difficult to predict forest productivity accurately across broad regions. While soil properties are not directly available from remote sensing data, they can potentially be inferred from linking these properties to observations that are readily available from satellite data, such as vegetation leaf area. We took advantage of the direct link that exists between above-ground productivity and maximum leaf area index (LAI_{max}) to derive and map soil fertility (FR) and available soil water storage capacity (ASWC) at 1 km resolution across forested areas in western North America. Initially, we generated estimates of LAI_{max} with a process-based growth model (3-PG), holding soil properties constant (FR = 50% of maximum, ASWC = 200 mm). To derive more realistic estimates of soil properties we inverted the model to infer FR and ASWC from iterative non-linear adjustments of the two soil properties so that model-predicted LAI_{max} values corresponded closely with MODIS-derived observations. We parameterized 3-PG for the most widely distributed tree species in the region, Douglas-fir. The resulting maps were notably more detailed than those derived from the globally available Harmonized World Soil Database. Among 51, level III ecoregions, and the ranges in the two soil properties tended to increase in parallel with LAI_{max}. Further improvements in the approach are envisioned by combining MODIS and LiDAR observations to extend the range and accuracy of LAI_{max} observations.

1. Introduction

Most regional and global-scale assessments of forest productivity ignore variation in soil properties because conventional soil maps are too coarse in scale, differ in nomenclature, and are inconsistent across political boundaries (Lathrop et al., 1995; Mulder et al., 2011; Zheng et al., 1996). Soil maps rarely take into account differences in the intensity of forest management (Canary et al., 2000), variation in atmospheric deposition (Talhelm et al., 2012), and biological fixation of nitrogen (Compton et al., 2003). In seasonally arid environments, both the fertility and water storage capacity of soils must be known to predict productivity accurately. How above-ground growth responds to increasing concentrations of atmospheric CO_2 also depends on soil fertility and the extent that drought alters the partitioning of resources below-ground (Hyvönen et al., 2007; Oren et al., 2001).

If process-based models are properly parameterized, and include information on soil properties, they can often predict annual growth of plantations within the errors of measurement (Almeida et al., 2004, 2009; Stape et al., 2004). Without such knowledge, predictions of productivity rarely account for more than 70% of the measured variation (Coops & Waring, 2001; Latta et al., 2010; Swenson et al., 2005). Clearly, more spatially accurate and consistent mapping of soil properties would be desirable.

What means are available to evaluate soil properties across large areas? One possible approach is to utilize the link between soils properties, climate, and productivity. While soil properties are not directly available at larger scales from remote sensing data, one possible approach to obtaining soil maps is from using their relationship to land surface properties that are readily available from satellite data, such as vegetation leaf area. For instance, within a region where the dominant life form of vegetation is similar, variation in canopy density, expressed as maximum leaf area index (LAI_{max}), is recognized as a surrogate of growth potential (Waring, 1983; Waring et al., 2005). The LAI_{max} is relatively insensitive to forest disturbance if other vegetation is allowed to grow (Goetz et al., 2006). In areas where water is readily available but nutrients are scarce, applications of fertilizer can more than double above-ground growth (Axelsson & Axelson, 1986; Stape et al., 2004). Likewise, where soils are fertile, but water is limited, LAI and productivity increase with irrigation (Stape et al., 2004). Where both water and nutrients are suboptimal, providing these resources in ample amounts may increase LAI by nearly 3-fold (Ryan et al., 1996).

Conceptually, we face a situation similar to that of hydrologists whom only have measurements of annual precipitation and stream

* Corresponding author. Tel.: +1 6048226452.
E-mail address: nicholas.coops@ubc.ca (N.C. Coops).

0034-4257/$ – see front matter © 2012 Elsevier Inc. All rights reserved.
http://dx.doi.org/10.1016/j.rse.2012.08.024

flow. They may assume that water vapor transfer to the atmosphere represents the difference between the two measured values. Further, if the density of vegetation varies, they might infer that the ratio of transpiration (T) to evaporation (E) will increase with LAI. In our case, we assume that difference between modeled and measured LAI_{max} is attributed to the two soil properties. Further, we expect that the importance of FR, compared with ASWC, will increase as climatic conditions favor an increase in LAI_{max}, regardless of the initial values selected for soil properties.

Since 1979, earth-orbiting satellites have provided a means of quantifying variation in LAI at various resolutions, spatially and temporarily (Cohen et al., 2002; Tucker, 1979). Most current satellite-derived estimates of LAI are imperfect. In sparse vegetation the reflectance spectra include background from soils and litter as well as the vegetation (Gao et al., 2000), and in dense vegetation the reflectance signal saturates below maximum values (Myneni et al., 2002). Despite these limitations, available global estimates of LAI, provide a spatially exhaustive and contiguous reference for comparison of values generated from process-based growth models and offer the possibility, through sensitivity analyses, of deriving reasonable estimates of soil fertility and available soil water storage capacity.

In this paper, we apply an iterative modeling approach across forested lands in western North America, where LAI_{max} is first modeled with fixed values of FR and ASWC and compared with satellite-derived values. Through further sensitivity analyses, incremental changes in the two soil properties are made until convergence is attained with MODIS LAI_{max}. The final products are mapped at a spatial resolution of 1 km across the forested component of 51, level III ecoregions included within the study area and compared with maps of related soil properties derived from other sources.

2. Data and methods

2.1. Description of study area

Across western North America, the distribution of flora is largely correlated with spatial variations in temperature and precipitation. Because of the mountainous terrain, climatic variation is extreme, with nearly the total range in forest productivity (3.0–25 Mg ha^{-1} yr^{-1}) and leaf area (0.5–10.0) recorded across a transect in western Oregon of <250 km (Runyon et al., 1994). Fig. 1 presents the distribution of 51, level III, ecoregions included within the study area. These include four broad subregions as indicated by color differences in Fig. 1.

The most productive subregion is included in the Marine West Coast Forest zone, which extends from Alaska in a progressively narrowing band to San Francisco. Western hemlock (*Tsuga heterophylla*) and Sitka spruce (*Picea sitchensis*) are present throughout most of this fog-belt defined zone, with Douglas-fir (*Pseudotsuga menziesii*), coast redwood (*Sequoia sempervirens*), Alaska yellow cedar (*Chamaecyparis nootkatensis*), western red cedar (*Thuja plicata*) and grand fir (*Abies grandis*) well represented in some areas.

The Northwest Forested Mountains is the second most productive subregion in the study area. Douglas-fir and western hemlock are abundant in mixtures with Pacific silver fir (*Abies amabilis*), noble fir (*Abies procera*) and western larch (*Larix occidentalis*). At higher elevations and latitudes, lodgepole pine (*Pinus contorta*), whitebark pine (*Pinus albicaulis*), mountain hemlock (*Tsuga mertensiana*), subalpine fir (*Abies lasiocarpa*), and Engelmann spruce (*Picea engelmannii*), are characteristic species.

On drier sites, ponderosa pine (*Pinus ponderosa*) and incense cedar (*Calocedrus decurrens*) are usually present. Ponderosa pine extends its range southward into the fringe of the North American Desert, with further reductions in productivity. In Oregon and northern California, in the rain shadow of the Cascade Mountains, open pine forests grade into western juniper (*Juniperus occidentalis*) woodlands and finally to sagebrush steppe (Franklin & Dyrness, 1973; Runyon et al., 1994). In the southwestern U.S., tree species make up only 2% of the flora, but include extensive stands of pinyon pine and juniper (McLaughlin, 1986).

Although the climate is extremely varied across the study area, the number of tree species is less than half that recorded in the Appalachian Mountains in the eastern part of the continent (Nightingale et al., 2008; Waring et al., 2006), with the most biological diversity in the Klamath Mountains (ecoregion 6.2.11) of southwestern Oregon and northwestern California (Whittaker, 1961). Two species, Douglas-fir (*P. menziesii*) and ponderosa pine (*P. ponderosa*), cover the widest array of forested environments in the study area (Little, 1971). We selected Douglas-fir as the most representative species of the two because its distribution covers more than 70% of the study area and the widest range in productivity (Hermann & Lavender, 1990).

2.2. Process-based growth model

There are a variety of physiologically-based process models available for use, however, only a few have been designed to scale projections of photosynthesis, evapotranspiration, structural growth, and mortality across landscapes (see reviews by Mäkelä et al., 2000; Nightingale et al., 2004). Among the most widely used is the 3-PG model (*P*hysiological *P*rinciples *P*redicting *G*rowth) developed by Landsberg and Waring (1997) which, when coupled with a decomposition model, provides estimates of net carbon exchange (Peng et al., 2002). 3-PG provides a compromise between highly complex, fine-temporal scale, process models, and those applied at annual time-steps. It is based on a number of established biophysical relationships and constants and incorporates simplifications that have emerged from studies conducted over a wide range of forests (Landsberg et al., 2003).

The basic model assumptions of 3-PG are as follows: a) monthly time-steps in climatic data are adequate to capture major trends, b) knowledge of the most limiting variable constraining photosynthesis each month is sufficient, c) autotrophic respiration (R_a) and net primary production (P_{net}) are approximately equal fractions of gross photosynthesis (P_g), d) maximum canopy conductance approaches a constant as LAI exceeds 3.0, and e) the proportion of photosynthate allocated to roots increases with drought and decreases with nutrient availability (Landsberg & Sands, 2010).

The 3-PG model calculates gross photosynthesis, transpiration, growth allocation and litter production at monthly intervals, and takes into account deficiencies in precipitation in previous months and years by sequentially up-dating a soil water balance. At monthly time steps, the model is unable to compute a snow water balance accurately, although one may assume that precipitation in months with average temperatures below freezing is in the form of snow. At annual time steps, the model sums monthly changes in tree number, mean diameter, stand basal area, above-ground volume and biomass, and updates changes in LAI.

In this study, we parameterized the 3-PG model using allometric data from conventional forestry yield tables and physiological observations from a range of previous studies, as summarized for Douglas-fir in Waring and McDowell (2002). To account for seasonal adjustments in temperature optima (Hember et al., 2010) and the genetic variation among populations of Douglas-fir, we broadened the range that photosynthesis could remain above 50% of maximum to lie between 0 °C and 35 °C by setting minimum, optimum, and maximum temperatures at −7 °C, 18 °C, and 40 °C, respectively. The photosynthetic response at temperatures < −2 °C was truncated to zero, because, below that threshold, stomata are generally closed (Hadley, 2000; Running et al., 1975). The fertility-dependent growth modifier in the 3-PG model is a function of the soil fertility rating, FR, which ranges between 0, for the poorest soils, and 1 for highly fertile soils (Landsberg & Waring, 1997). Landsberg and Sands (2010) define

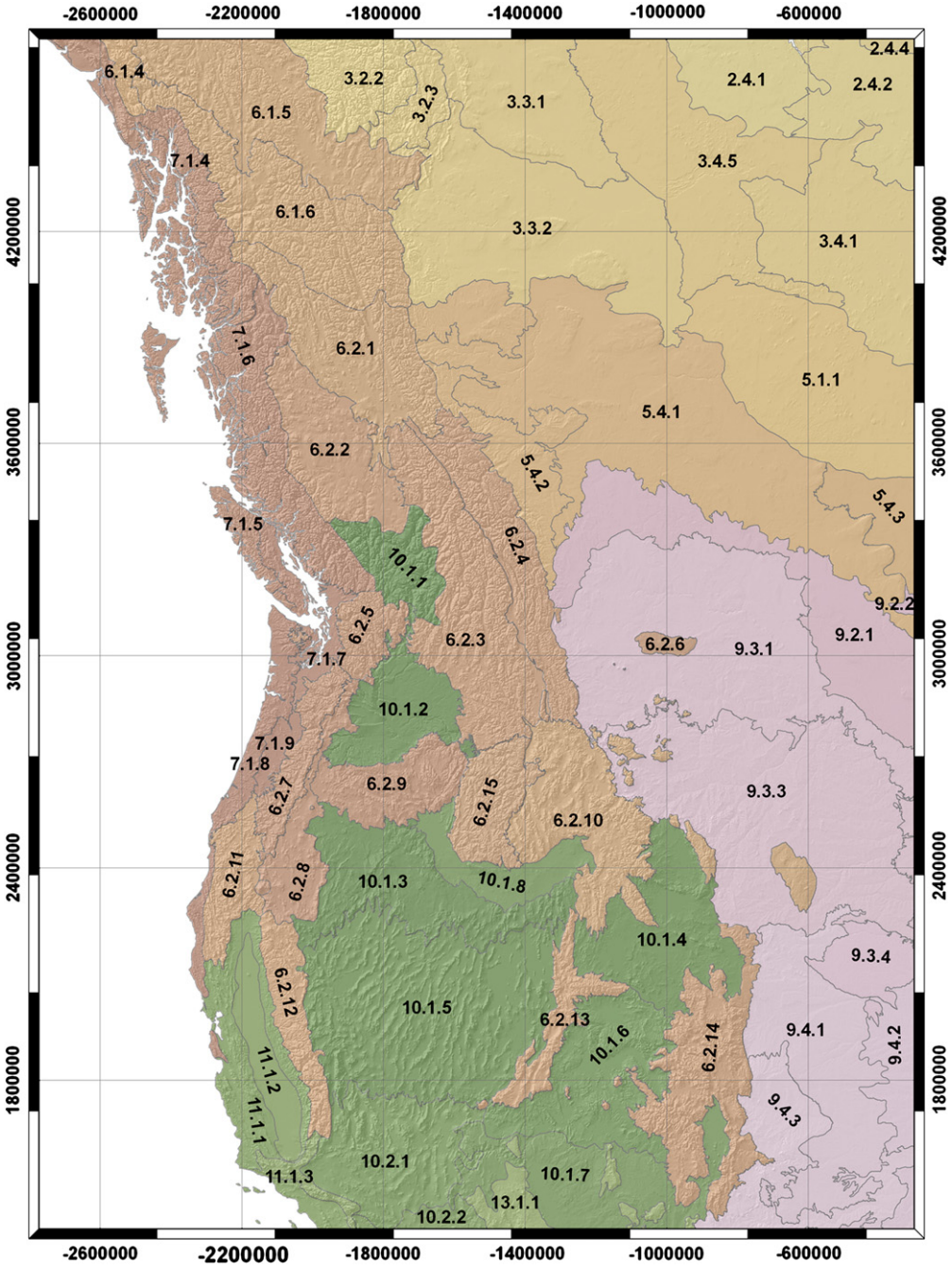

Fig. 1. Spatial distribution of 51 U.S. Environmental Protection Agency (EPA) level III ecoregions, identified by number in the study area. Refer to Tables 1 and 2 for more detail. Different colors represent level I designated ecoregions. Gray corresponds to areas of no forest. (For interpretation of the references to color in this figure legend, the reader is referred to the web version of this article.)

soil fertility as a site property and therefore the same for all species. Differences among species in their response are incorporated into the process-based model by altering how quantum efficiency is changed and the way that growth is allocated above- and below ground. Soil fertility is difficult to assess through any set of static soil analyses because growth is restricted by the flux of nutrients to roots, not the concentration per se (Ingestad, 1982). The most productive sites, with a long growing season and adequate water, place the highest demand for nutrients from the soil. Sites with lower productivity exert less demand and usually for much shorter durations, i.e., primarily when conditions are favorable for shoot elongation. It is at such times, when growth potential is highest, that soil fertility is best assessed (Waring & Youngberg, 1972). This usually corresponds to when LAI is near its maximum value. We set soil fertility to vary over its full range between 0 and 1, with direct coupling to canopy quantum efficiency (α), which was assumed to vary between 0.02 and 0.055 mol C/ mol photon (1.1 to 3.03 gC MJ^{-1}) absorbed photosynthetically active radiation. AWSC was allowed to vary between 0 and 300 mm (Waring & McDowell, 2002).

2.3. Climatic data

To obtain climate surfaces over the region we utilized interpolations of climate station data produce using non-linear adjustments for mountainous terrain as produced and described by Hamann and Wang (2005). The weather observations used by Hamann and Wang (2005) were acquired from thousands of stations irregularly distributed throughout the region and interpolated spatially using Climate-WNA

(http://www.genetics.forestry.ubc.ca/cfcg/ ClimateWNA/ClimateWNA.html). A 90 m-Digital Elevation Model (DEM), obtained from the Shuttle Radar Topography Mission (SRTM), was converted to 1 km to provide comparable spatial data with climatic extrapolations. We utilized surfaces developed using 2000 data onwards.

Mean monthly daytime vapor pressure deficits (D) were estimated by assuming that the water vapor concentrations present throughout the day would be equivalent to those that would be obtained if the mean minimum temperature is assumed equal to the mean dew point temperature (Landsberg & Sands, 2010). Because humidity deficits exceed a stomata-closing threshold of >2.5 kPa (Waring & Franklin, 1979) in the most arid savannas (Plaut et al., 2012), no adjustments were made to compensate for conditions where the humidity did not reach 100% at night (Kimball et al., 1997). The maximum D was calculated each month as the difference between the saturated vapor pressure at the mean maximum and minimum temperatures. Mean daytime D was calculated at two thirds of the maximum value (Waring, 2000).

The number of days per month with subfreezing temperatures (≤2 °C) was estimated from empirical equations with mean minimum temperature (Coops et al., 1998). In modeling, we did not attempt to account for extremes in temperature that might kill native species because chances of such events are low, given that most tree species in the region can exceed 500 years of age under natural conditions (Schulman, 1954; Waring & Franklin, 1979).

Monthly estimates of total incoming short-wave radiation were calculated using a modeling approach detailed by Coops et al. (2000) where the potential radiation reaching any spot is first calculated and then reduced, based on the clarity (transmissivity) of the atmosphere. Changes in the atmospheric transmissivity are mirrored in temperature extremes (Bristow & Campbell, 1984). With a digital elevation model, we adjusted for differences in slope, aspect, and elevation as well as for variations in the fraction of diffuse and direct solar beam radiation (Hungerford et al., 1989). Relative to direct measurements, modeled values of the direct and diffuse components of incident solar radiation were predicted with 93–99% accuracy on flat surfaces and accounted for >87% of the observed variation, with a mean error<2 MJ m^{-2} day^{-1}, on sloping terrain (Coops et al., 2000).

2.4. MODIS leaf area index

Satellite-derived estimates of leaf area index were obtained from the MODIS Collection 5 LAI (MOD15A2) global products over nearly a decade, beginning in year 2000 day 49 and ending in year 2009 day 361. The MODIS LAI product is derived every 8 days at 1 km spatial resolution (Knyazikhin et al., 1998). The algorithm has been compared to field observations across a wide range of biomes and conditions in the past decade (Cohen, 2003; Gu et al., 2006; Myneni et al., 2002; Weiss et al., 2007; Zhang et al., 2003). We used a recently re-processed MODIS v5 LAI dataset that provides improved estimates by filtering out low quality images and by imposing a time-series analysis with TIMESAT software (Jönsson & Eklundh, 2004) to confirm instrument calibration (Yuan et al., 2011). From this dataset we computed the maximum annual LAI_{max} for each year from 2000 to 2009 and then averaged these values for each pixel over the period. Forested or woodland areas across the study area were defined using the MODIS-derived UMD (University of Maryland) land cover classification scheme.

2.5. Inversion of 3-PG

When run in the regular (forward) mode, 3-PG predicts growth potential (here referred to as LAI_{max}) as a function of FR and ASWC. In the inverted model, FR and ASWC can be derived, if the growth potential is known. In our approach, we assume that the MODIS-derived LAI_{max} values represent the current growth potential at each pixel, therefore FR and ASWC can be derived from inverse modeling of 3-PG. The inversion process seeks to minimize the difference between forward modeled and observed data (here LAI_{max}) by adjusting the model input (FR and ASWC) iteratively based on a priori knowledge to allow 3-PG estimates of LAI_{max} to converge on values derived from MODIS. This kind of model inversion is described mathematically by Verstraete et al. (1996) as a non-linear minimization problem. Different algorithms are available for inversion of non-linear models, with the choice based on their relative efficiency in minimizing the residuals between forward modeled (here: 3-PG estimates of LAI_{max}) and measured observations (here: MODIS LAI_{max}).

In this study, we selected a trust-region-reflective algorithm based on the interior-reflective Newton method (Coleman & Li, 1996; Coleman et al., 2002). The algorithm allows us to define the range in data to reasonable values (FR = 0–1.0; ASWS = 0–300 mm). While this technique is well suited to infer multiple inversion products simultaneously, one limitation is that it may generate values that converge on the maximum value of one of the desired products (ASWC or FR), especially if the inversion variable (LAI_{max}) is too uniformly distributed. To mitigate this problem, if it occurred, we implemented a two-step backup algorithm to infer ASWC and FR within a 3×3 pixel moving window.

The iterative procedure was implemented in a series of steps. We first tried to solve for FR and ASWC simultaneously, assuming initial values of FR (0.5) and AWSC (200 mm).Where estimates of LAI_{max} did not converge, we next assumed for areas with $LAI_{max}<3$ that water was likely to be more limiting than fertility, based on field measurements of plant water stress and LAI_{max} across a transect in Oregon (Runyon et al., 1994). Hence we solved for ASWC with FR set at 0.60. Similarly, for areas with $LAI_{max}\geq 3$, FR was designated the most important of the two soil properties, and derived by setting ASWC at 170 mm. In a final step, the less sensitive of the two soil properties was derived by holding the value obtained in step one constant. In all simulations, the 3-PG model was initialized with 1000 seedlings per hectare and allowed to grow trees for 50 years under averaged monthly climatic conditions for the period 2000–2009.

2.6. Comparable soil data

We have already pointed out that accurate regional information on soil properties in a form required for modeling rarely exists, particularly across political boundaries. Moreover, because the scale of most regional and continental soil maps ranges from 1:500,000 to 1:1,000,000, much of the heterogeneity in soils is obscured (Landsberg & Coops, 1999). One of the few sources of comparable data across the western portion of North America is that derived from the Harmonized World Soil Database (HWSD), which is a compilation of existing regional and national soil information at a 1:5,000,000 scale acquired from the FAO-UNESCO Soil Map of the World (FAO, 1971–1981 http://www.fao.org/nr/land/soils/digital-soil-map-of-the-world/en/). The dataset over North America is primarily the same as the FAO soil map of the world (i.e., with a spatial resolution of 1 km (30 arc seconds)) and was designed to be useful to those charged with assessing crop yields and response to climate change within recognized agricultural and ecological zones (Batjes, 2011).

Within the standardized GIS structure of the HWSD, we extracted estimates of water storage capacity and soil depth, and organic carbon content in the upper horizons and subsoil, to a maximum depth of 1 m. In the case of soil water capacity, estimates were available in 5 classes defined in 25 mm intervals between 50 and 150 mm with a 6th class representing ≤15 mm/m. Organic carbon, averaged for each soil horizon down to a maximum depth of 1 m, served as an index of soil fertility on well drained sites (Batjes, 2011). Similar to our treatment of soil water storage capacity, the organic carbon data were separated into 4 classes 0.2–0.6, 0.61–1.2, 1.21–2.0 and

> 2.0 %. Soils that are extremely low in organic carbon (<0.2%) require enrichment with organic or inorganic fertilizer to be at all productive; soils with an organic matter content of less than 0.6% are also considered infertile for agriculture. Although the ratio of carbon to nitrogen in soils approaches a constant for similar types of vegetation (Zinke & Strangenberger, 2000), the relation between total nitrogen and that available to plants is logarithmic (Swenson et al., 2005).

3. Results

Fig. 2(a) contrasts 3-PG predicted LAI_{max} using fixed soil properties to those derived from MODIS (2b). General agreement is shown between the two estimates for the highly productive forests in the Pacific Northwest and the least productive areas in Canada and across much of the southwestern U.S. Large differences between the two estimates of LAI_{max} are apparent in the Sierra Mountains of California, portions of Rocky Mountains, and elsewhere. If we assume that LAI_{max} is truly represented from MODIS, then large differences between modeled and measured LAI_{max} reflect significant variation from one or both of the default soil properties used in the initial runs with 3-PG.

Fig. 3 presents maps of (a) soil fertility and (b) available soil water storage capacity created in this project, derived from the iterative inversion process described in Section 2.5. It can be seen, by comparing the map of MODIS-derived LAI_{max} in Fig. 2 with the derived values for (a) FR and (b) ASWC in Fig. 3, that the most productive sites in the Pacific Northwest Region not only have favorable climates but also relatively deep and fertile soils. In contrast, much of the forested land east of the crest of the Cascade and Sierra Mountains receives sparse rainfall and endures hot, dry summers. In these regions, LAI_{max}

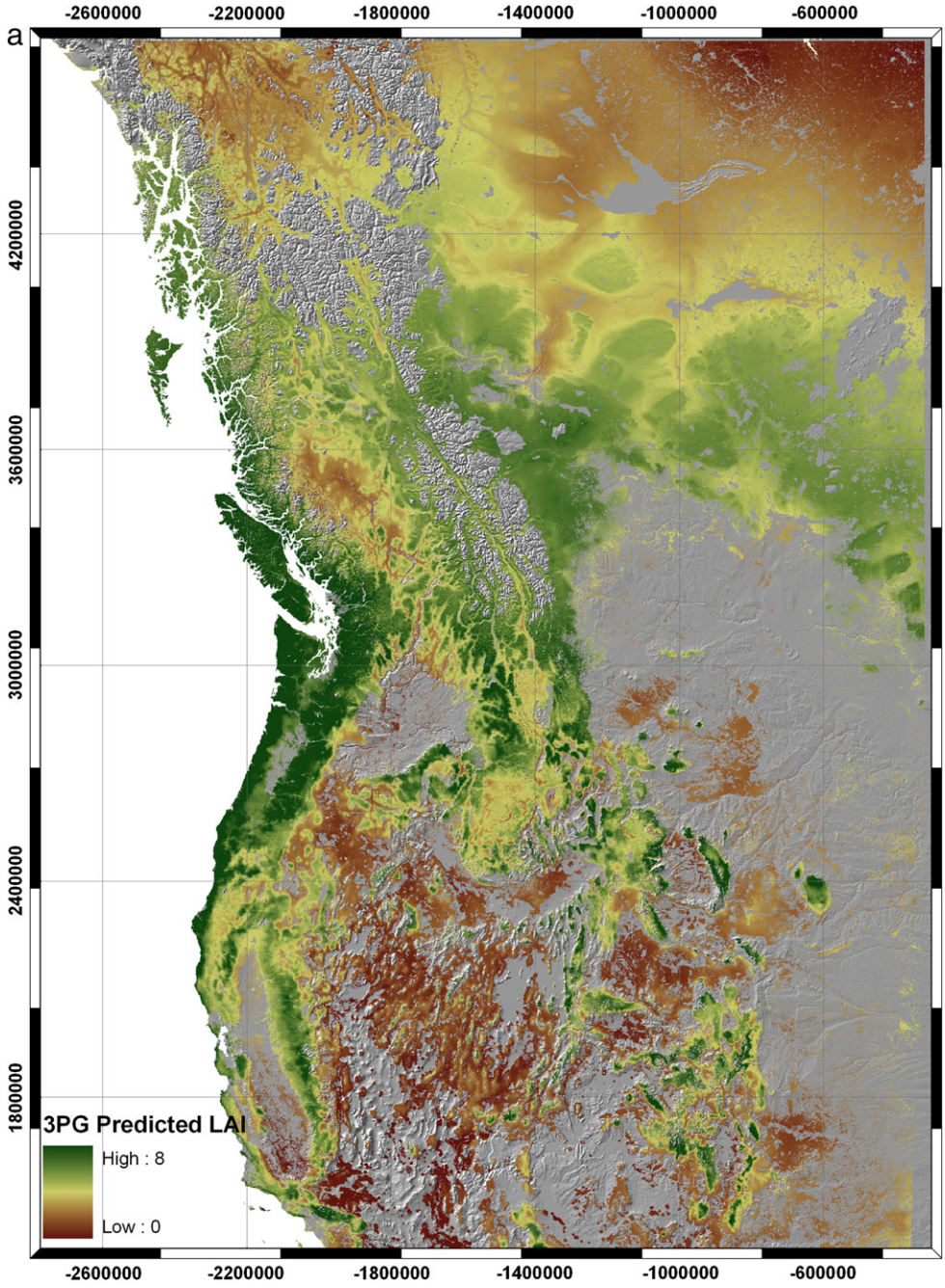

Fig. 2. Contrast between predicted and satellite-derived estimates of leaf area index (LAI). (a) Simulated for forested areas with 3-PG with soil fertility at 50% of maximum and ASWC at 200 mm. (b) LAI_{max} derived from MODIS over the period from 2000 to 2009.

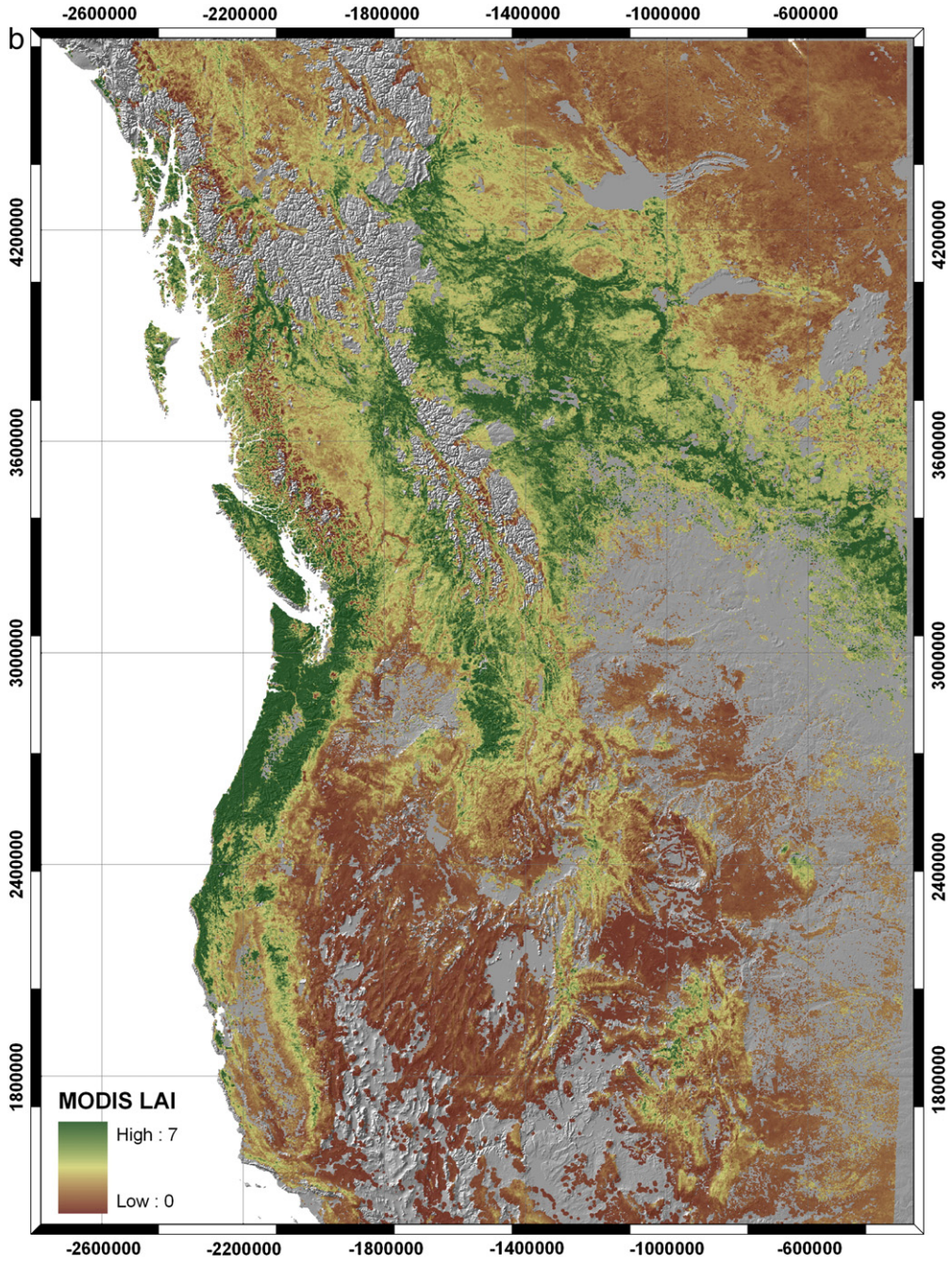

Fig. 2 (*continued*).

is generally <2.0 and the majority of soils are relatively infertile and often shallow. More details on the range of soil properties in each of the 51 level III ecoregions are provided in Tables 1 and 2. The basic trends in FR and ASMC depicted in Fig. 3 are supported by the coarse-scale maps of soil properties acquired from the Harmonized World Soil Database shown in Fig. 4(a) and (b).

4. Discussion

4.1. Relative importance of the two soil properties

In areas where precipitation is sufficient to support LAI_{max} values > 3.0, drought, if it does occur, generally lasts for only a few months (Runyon et al., 1994). In such cases, soil fertility largely determines the height growth and density of vegetation, because, at the more drought-prone sites, the growing season starts early with fully water-charged soils (Waring & Cleary, 1967; Waring & Major, 1964; Waring & Youngberg, 1972). In the 3-PG model, as FR increases, the quantum efficiency increases linearly, up to 3-fold. That response makes photosynthesis per unit of leaf area highly sensitive to soil fertility, assuming that other factors do not severely limit the process. On the other hand, ASWC affects photosynthesis only when water is considerably depleted in the soil profile. Both soil properties, when suboptimal, shift the limited amounts of photosynthate available away from above- to below-ground production (Landsberg & Waring, 1997).

In areas where precipitation is severely limited, such as the pinyon pine-juniper woodlands in the southwestern U.S., photosynthesis is often water limited for more than half the year, although the LAI_{max} is generally below 1.5 (Peterman et al., 2012). The soils lack organic matter and are generally infertile. To a somewhat lesser degree,

ponderosa pine, which supports an LAI_{max} usually <2.5, is also a vegetation type where water limitations exceed that imposed by soil fertility (Coops et al., 2005). These observations highlight the significance of the threshold value of LAI_{max} at 3.0. It could be argued that ponderosa pine would be a more representative species than Douglas-fir, particularly in the more arid parts of the study area. However, preliminary comparisons of the two species on sites with LAI_{max} ranging from 1.0 to 10.0 m^2 m^{-2} were found in close (± 0.5) agreement (unpublished).

4.2. Comparisons with broad soil surveys

Our mapping of soil fertility in Fig. 3 shows considerably more detail than that provided in HWSP product (Fig. 4). In part, this reflects the definition of only 4 classes of soil carbon content in the latter, as well as a coarser spatial resolution. Swenson et al. (2005) refined the link between soil carbon content and available nitrogen across forested areas in the west-coastal state of Oregon, producing a map that showed much closer agreement between FR predictions within that part of the study area (Fig. 3). The wide range in FR reported in Table 1 for southwestern Oregon (Klamath Mountain ecoregion, 6.2.11) is a reflection of differences in underlying parent materials, which range from infertile serpentine-derived soils to those derived from graphite schist with ammonium in the parent material (Dahlgren, 1994). All ecoregions had some soils mapped as infertile, but only those able to support values of $LAI_{max} > 6.0$ (Fig. 3) ranked high in FR (i.e., >0.6) in Table 1. Most of the ecoregions with high values of FR are located in the northwestern part of the United States

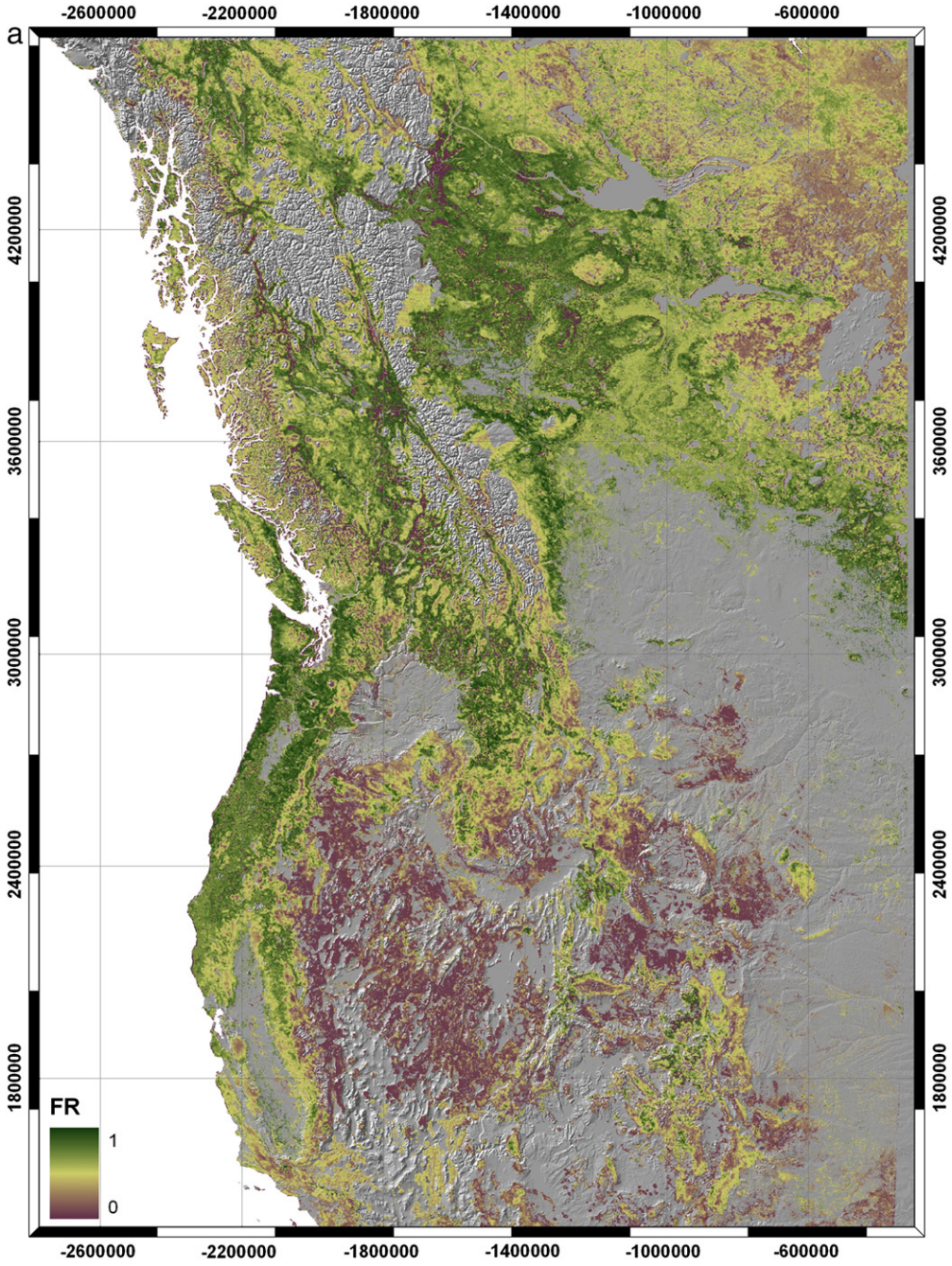

Fig. 3. Values derived with the 3-PG model under average climatic conditions (2000–2009) for (a) soil fertility (FR), and (b) available soil water holding capacity (ASWC) across forested zones in the study area.

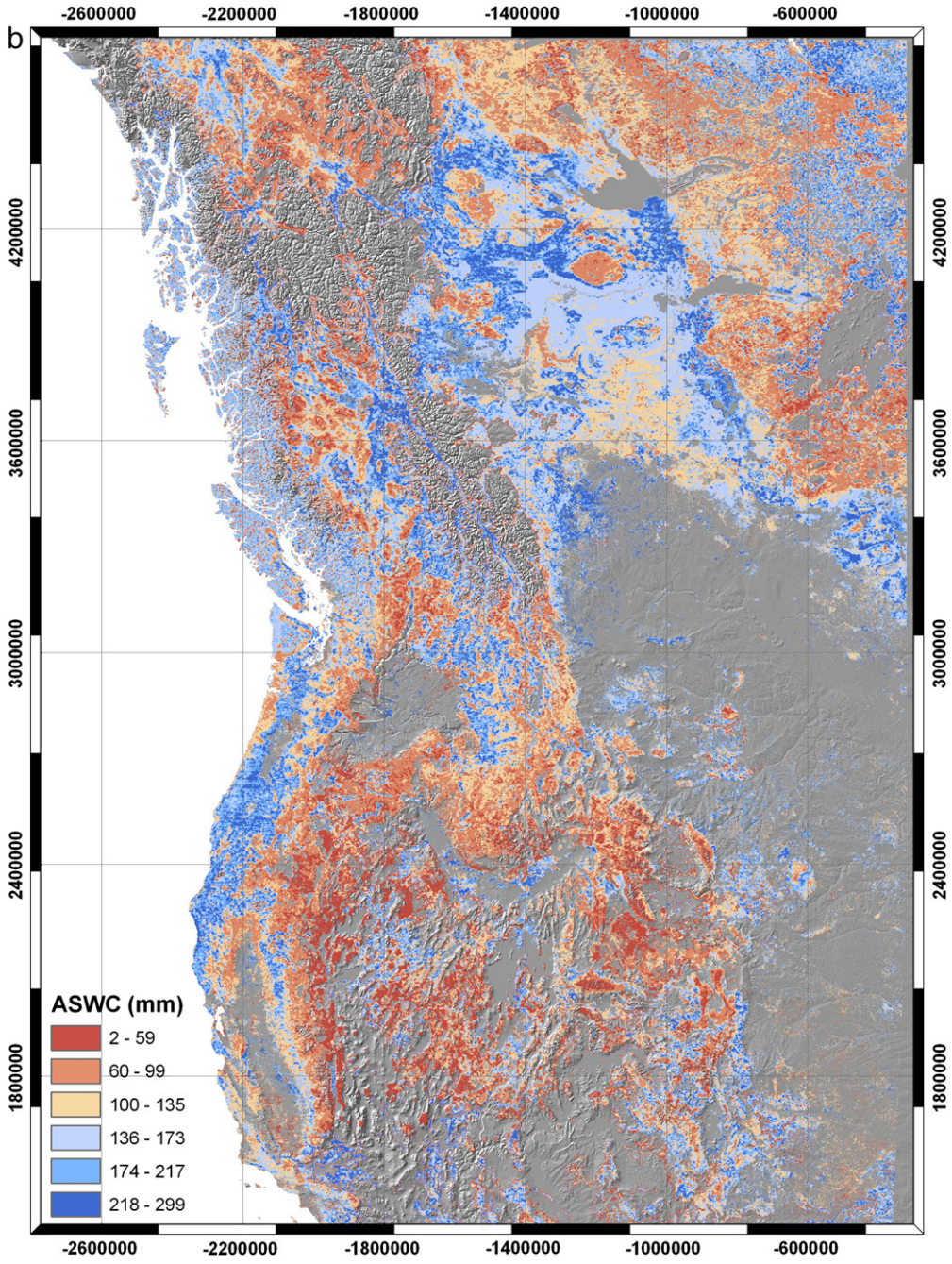

Fig. 3 (*continued*).

and in parts of British Columbia and Alberta (Fig. 1). We believe that some soils in the Coast Ranges of Oregon and Washington, where nitrogen-fixing species of *Alnus* dominate following disturbance, are much more fertile than represented in Fig. 3, but this is masked in our analysis because LAI_{max} above 7.0 cannot be discriminated with passive remote sensing (Myneni et al., 2002).

The HWSD maps of ASWC (Fig. 4) show much closer general agreement with our classification than was the case with FR (Fig. 3). The maximum value of 150 mm in the HWSD classification is a reflection of limiting the analyses to the depth of 1.0 m. Our maps delineate values up to 300 mm, which are more realistic, given that trees even in the Coast Range of Oregon can extend their roots to >2 m depth. Transpiration rates there average 3 mm day^{-1} during the dry summer months, if limited by drought, would not be able to support observed growth rates (Waring et al., 2008).

4.3. Forecasted improvements in monitoring LAI_{max}

Methods to predict LAI_{max} from optical remote sensing imagery, such as MODIS rely on the spectral response characteristics of green leaves compared with other land surface materials (Zheng & Moskal, 2009). As a result, the effect of the background soil, atmosphere and viewing directions can all impact the accuracy of LAI predictions. While 250 m spatial resolution data can help minimize some of these effects, the LAI estimates do still only provide regional estimates of LAI. In addition however the optical prediction of LAI becomes saturated at LAI_{max} values > 7.0. Because LAI_{max} values can extend in the field to 10 and even 12 m^2 m^{-2} (Waring, 2000), the iterative modeling approach is unable to discriminate the most fertile soils and productive sites with passive remote sensing. Airborne LiDAR has the ability to quantify the full range in LAI_{max} (Lefsky et

Table 1
Range in simulated values of soil fertility (FR) among 51 ecoregions.

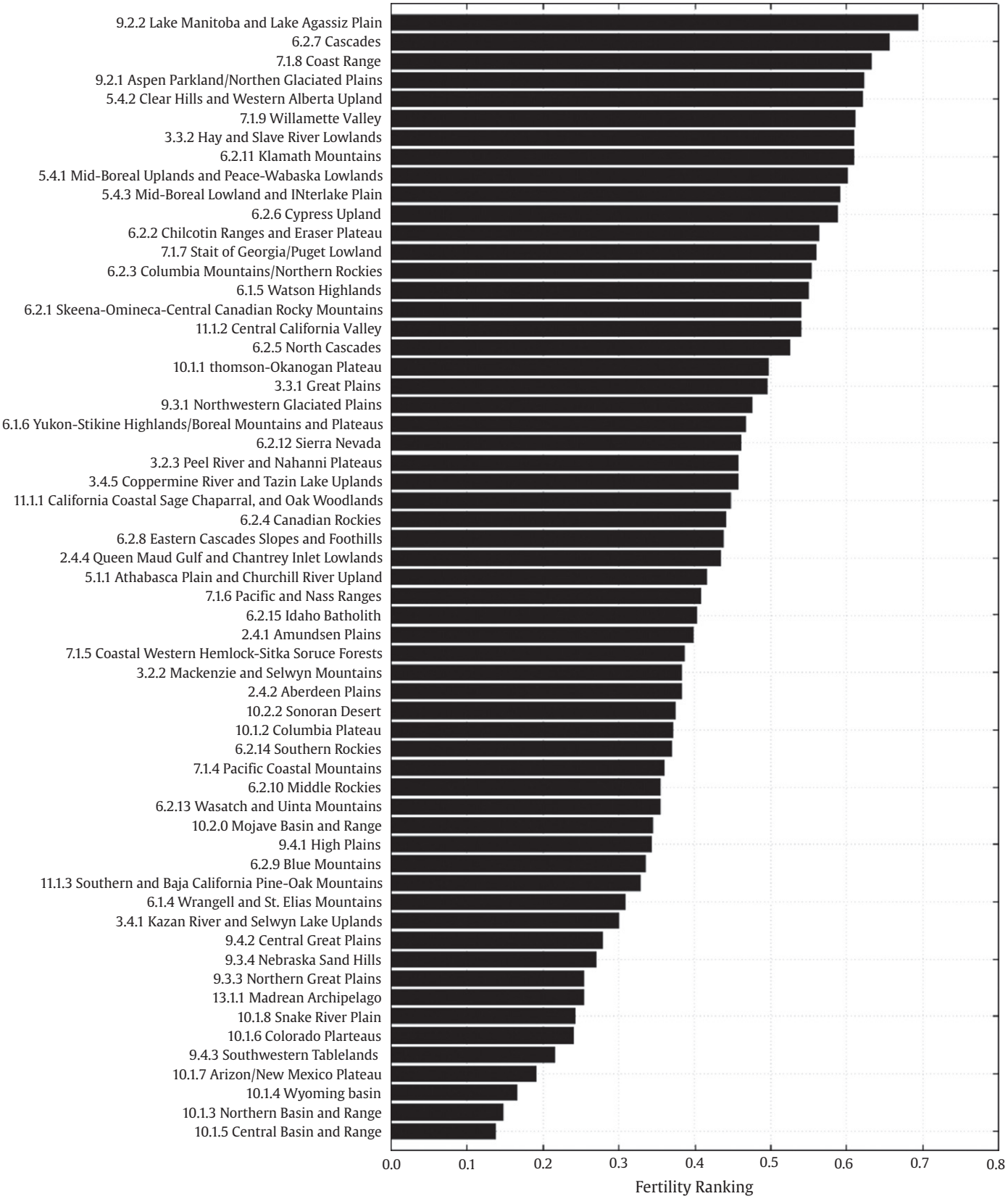

Table 2
Range in simulated values available soil water storage capacity (ASWC) among 51 ecoregions.

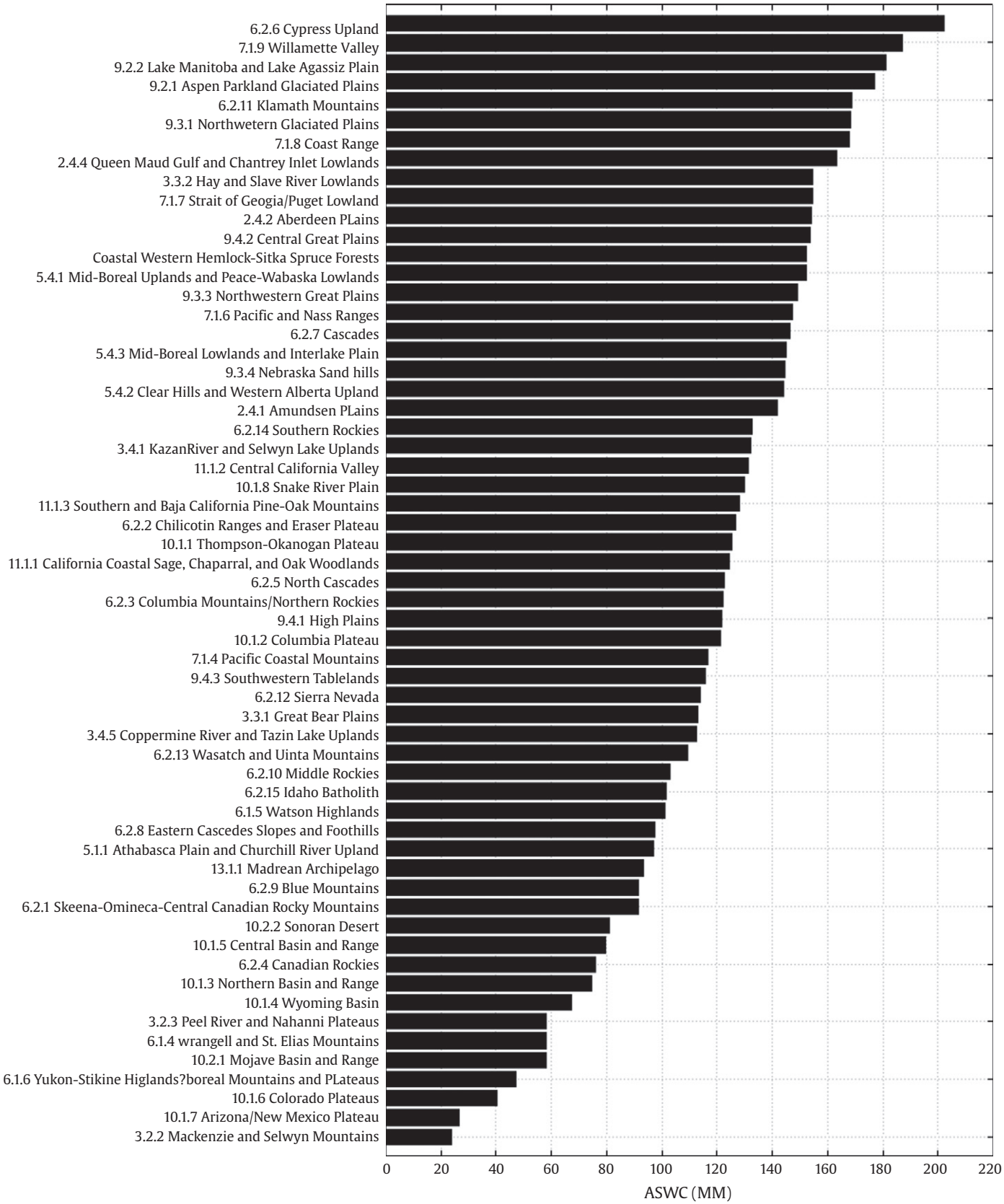

al., 2002), and recently, in combination with MODIS, satellite-borne LiDAR has also aided in providing the first world-wide estimates of tree heights and above-ground biomass (Lefsky, 2010; Tollefson, 2009).

4.4. Weaknesses in the approach

We are not under the illusion that the maps produced in Fig. 3 are truly accurate, although the classifications appear reasonable where we have on-the-ground experience. We also know, from direct measurements of tree water potentials and transpiration, that ASWC must be assessed on forested soils to a depth much deeper than 1 m (Jackson et al., 2000). Where soil maps accurately assess ASWC, it is possible to predict tree mortality to drought-related bark beetle attacks with considerable accuracy (Peterman et al., 2012).

Another weakness in the current approach is the assumption that LAI_{max} is actually reached where insects, pathogens, fire, and logging continue to disturb forests. More detailed analyses over longer periods should help, along with improved instruments to quantify variation in LAI, however the launch of the MODIS sensor in 1999 and 2002 limits this type of analysis using this sensor to only from those times forward. Other longer-term datasets do exist, such as NOAA AVHRR data, however calibration and prediction of LAI from these sensors are more problematic.

The spatial extrapolation procedures used to provide the climatic drivers, and simplifications in the 3-PG model itself, combine to limit the accuracy in predicting LAI_{max}. Similarly, the parameterization of 3-PG for Douglas-fir growing in a coastal environment (Waring & McDowell, 2002) is unlikely to represent the genetic variation across the entire study area. In future applications of the approach, we propose

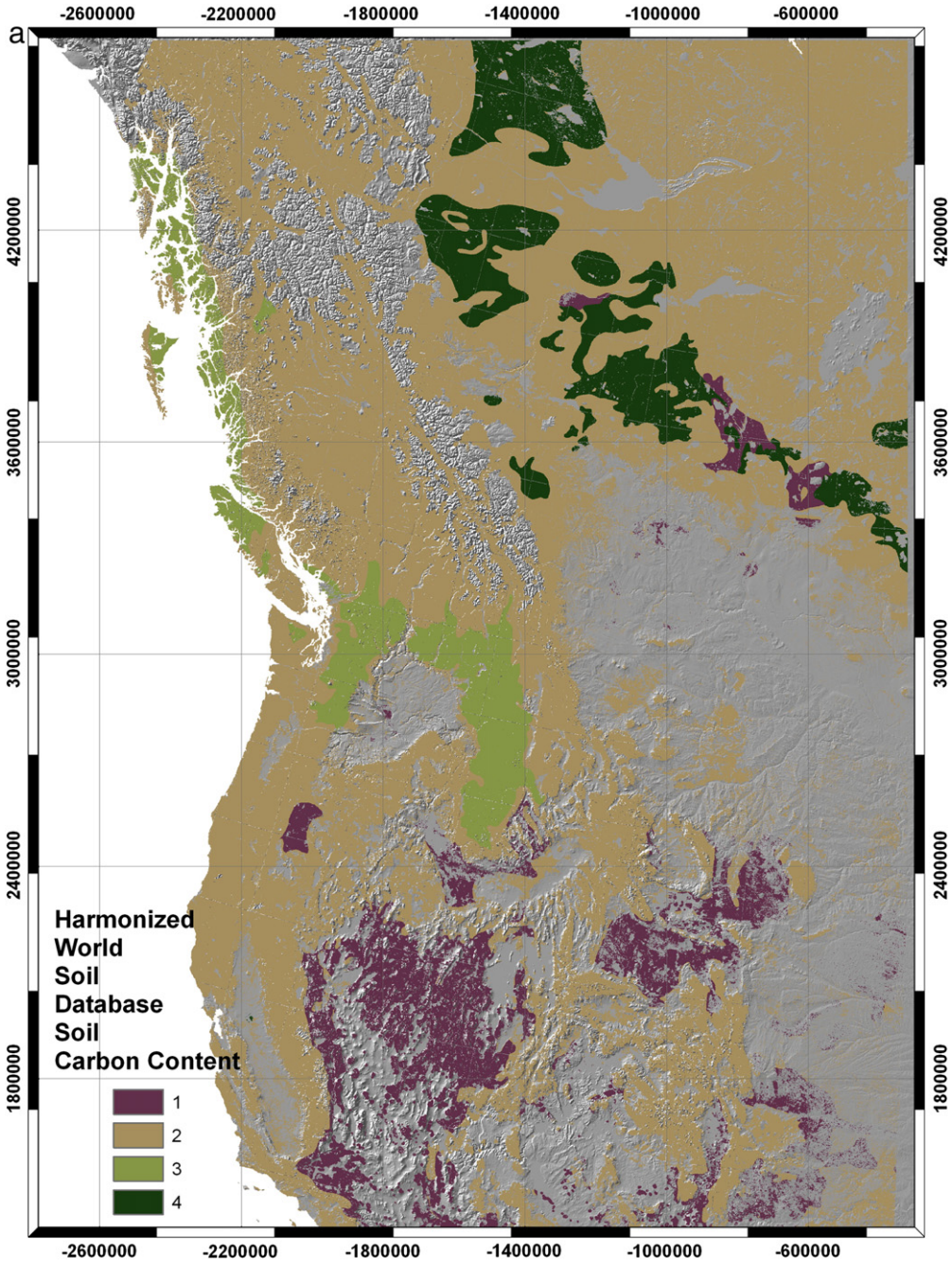

Fig. 4. Coarse-scale 1:5,000,000 maps provided by the Harmonized World Soil Database (a) soil carbon content classes (4 classes: 0.2–0.6, 0.61–1.2, 1.21–2.0 and >2.0 %) and (b) available soil water storage capacity (mm, to depth of 1 m) for forested zones within the study area.

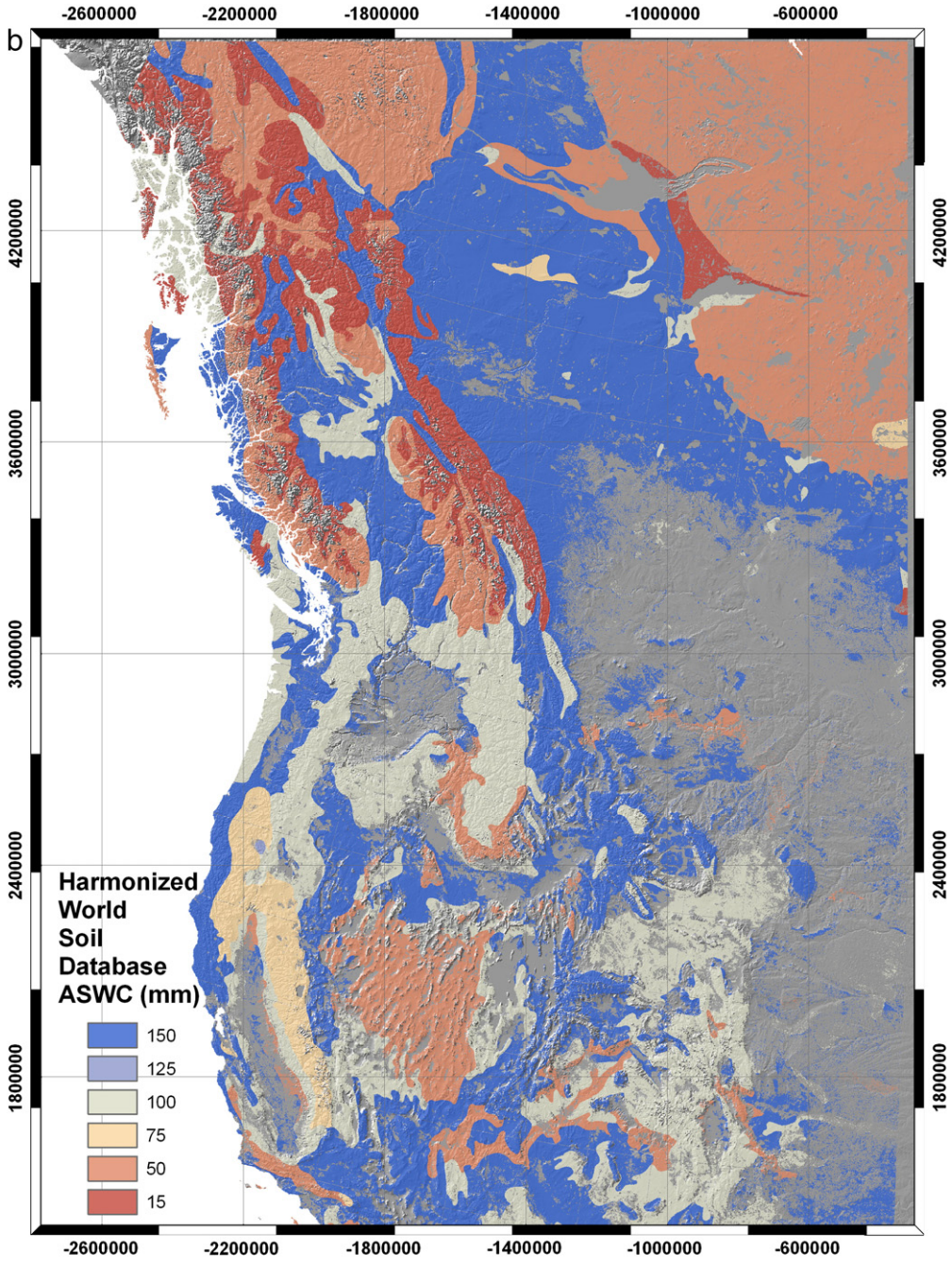

Fig. 4 (*continued*).

to compare results using additional species (e.g., ponderosa pine). We hope that others will test the approach locally with different species, more refined models, and higher spatial resolution.

5. Conclusion

A real need exists for improved maps of soil properties to model the impact of changing climate, rising levels of atmospheric CO_2, and nitrogen deposition on forests. We took advantage of a general linear relation that exists between LAI_{max} and forest productivity to estimate soil fertility and available soil water storage capacity across western North America at 1 km spatial resolution. In doing this, an optimization technique was utilized that adjusts estimates of FR and ASWC to match values of LAI_{max} derived from NASA's MODIS instrument. The resulting maps showed a general increase in both soil properties with increasing LAI_{max}. Further improvements in the approach require increased accuracy in satellite-derived estimates of forest growth and LAI, as well as wider testing of the approach in specific areas.

Acknowledgments

J.J. Landsberg suggested this approach to us some years ago. He and W. Peterman also provided useful comments on an earlier draft of this paper. We are grateful to Dr Fabio Fontana for help in compiling the re-processed MODIS LAI archive. This study was supported by the National Aeronautics and Space Administration (NASA Grant NNX09AR59G) to Waring as part of the Biodiversity and Ecological Forecasting program and a Canadian NSERC Discovery grant to Coops. We also acknowledge support of Hilker from Goddard Space Flight Center, NASA.

References

Almeida, A. C., Landsberg, J. J., & Sands, P. J. (2004). Parameterisation of 3-PG model for fast-growing *Eucalyptus grandis* plantations. *Forest Ecology and Management*, *193*, 179–195.

Almeida, A., Sands, P. J., Bruce, J., Siggins, A. W., Leriche, A. J., Battaglia, M., et al. (2009). Use of a spatial process-based model to quantify forest plantation productivity and water use efficiency under climate change scenarios. *18th World IMACS/MODSIM Congress, Cairns, Australia* (http://mssanz.org.au/modsim09)

Axelsson, E., & Axelson, B. (1986). Changes in carbon allocation patterns in spruce and pine trees following irrigation and fertilization. *Tree Physiology*, *2*, 189–204.

Batjes, N. H. (2011). Soil organic carbon stocks under native vegetation — Revised estimates for use with the simple assessment option of the Carbon Benefits Project system. *Agricultural, Ecosystems & Environment*, *142*, 365–373.

Bristow, K. L., & Campbell, G. S. (1984). On the relationship between incoming solar radiation and daily maximum and minimum temperature. *Agricultural and Forest Meteorology*, *31*, 156–166.

Canary, J. D., Harrison, R. B., Compton, J. E., & Chappell, H. N. (2000). Additional carbon sequestration following repeated urea fertilization of second-growth Douglas-fir stands in western Washington. *Forest Ecology and Management*, *138*, 225–232.

Cohen, W. B. (2003). Comparisons of land cover and LAI estimates derived from ETM+ and MODIS for four sites in North America: A quality assessment of 2000/2001 provisional MODIS products. *Remote Sensing of Environment*, *88*, 233–255.

Cohen, W. B., Spies, T. A., Alig, R. J., Oetter, D. R., Maiersperger, T. K., & Fiorella, M. (2002). Characterizing 23 years (1972–95) of stand replacement disturbance in western Oregon forests with Landsat imagery. *Ecosystems*, *5*, 122–137.

Coleman, T. F., & Li, Y. Y. (1996). An interior trust region approach for nonlinear minimization subject to bounds. *SIAM Journal on Optimization*, *6*, 418–445.

Coleman, T. F., Liu, J. G., & Yuan, W. (2002). A new trust-region algorithm for equality constrained optimization. *Computational Optimization and Applications*, *21*, 177–199.

Compton, J. E., Church, M. R., Larned, S. T., & Hogsett, W. E. (2003). Nitrogen export from forested watersheds in the Oregon Coast Range: The role of N_2-fixing red alder. *Ecosystems*, *6*, 773–785.

Coops, N. C., & Waring, R. H. (2001). Estimating maximum potential site productivity and site water stress of the eastern Siskiyous using 3-PGS. *Canadian Journal of Forest Research*, *31*, 143–154.

Coops, N. C., Waring, R. H., & Landsberg, J. J. (1998). Assessing forest productivity in Australia and New Zealand using a physiologically-based model driven with averaged monthly weather data and satellite derived estimates of canopy photosynthetic capacity. *Forest Ecology and Management*, *104*, 113–127.

Coops, N. C., Waring, R. H., & Law, B. E. (2005). Assessing the past and future distribution and productivity of ponderosa pine in the Pacific Northwest using a process model, 3-PG. *Ecological Modelling*, *183*, 107–124.

Coops, N. C., Waring, R. H., & Moncrieff, J. B. (2000). Estimating mean monthly incident solar radiation on horizontal and inclined slopes from mean monthly temperature extremes. *International Journal of Biometeorology*, *44*, 204–211.

Dahlgren, R. A. (1994). Soil acidification and nitrogen saturation from weathering of ammonium-bearing rock. *Nature*, *368*, 838–841.

Franklin, J. F., & Dyrness, C. T. (1973). *Natural vegetation of Oregon and Washington*. Oregon, USA: Oregon State University Press.

Gao, X., Huete, A. R., Ni, W., & Miura, T. (2000). Optical–biophysical relationships of vegetation spectra without background contamination. *Remote Sensing of Environment*, *74*, 609–620.

Goetz, S. J., Fiske, G. J., & Bunn, A. G. (2006). Using satellite time-series data sets to analyze fire disturbance and forest recovery across Canada. *Remote Sensing of Environment*, *101*, 262–366.

Gu, Y., Belair, S., Mahfouf, J., & Deblonde, G. (2006). Optimal interpolation analysis of leaf area index using MODIS data. *Remote Sensing of Environment*, *104*, 283–296.

Hadley, J. L. (2000). Effect of daily minimum temperature on photosynthesis in eastern hemlock *Tsuga canadensis* L. in autumn and winter. *Arctic, Antarctic, and Alpine Research*, *32*, 368–374.

Hamann, A., & Wang, T. (2005). Models of climate normal for genecology and climate change studies in British Columbia. *Agricultural and Forest Meteorology*, *128*, 211–221.

Hember, R. A., Coops, N. C., Black, T. A., & Guy, R. D. (2010). Simulating gross primary production across a chronosequence of coastal Douglas-fir stands with a production efficiency model. *Agricultural and Forest Meteorology*, *150*, 238–253.

Hermann, R. K., & Lavender, D. (1990). Pseudotsuga menziesii (Mirb.) Franco Douglas-fir. *In Silvics of North America Vol. 1, Conifers.* USDA Forest Service (Publ.), pp. 527–540.

Hungerford, R. D., Nemani, R. R., Running, S. W., & Coughlan, J. C. (1989). MT-CLIM. A mountain microclimate simulation model. *USDA Forest Service Research Paper INT-414, Ogden, Utah*.

Hyvönen, R., Ågren, G., Linder, S., Persson, Cotrufo, M. F., Ekblad, A., et al. (2007). The likely impact of elevated CO_2, nitrogen deposition, increased temperature and management on carbon sequestration in temperate and boreal forest ecosystems: A literature review. *New Phytologist*, *173*, 463–480.

Ingestad, T. (1982). Relative addition rate and external concentration; driving variables used in plant nutrition research. *Plant, Cell & Environment*, *5*, 443–453.

Jackson, R. B., Sperry, J. S., & Dawson, T. E. (2000). Root water uptake and transport: Using physiological processes in global predictions. *Proceedings of the National Academy of Science*, *5*, 482–488.

Jönsson, P., & Eklundh, L. (2004). TIMESAT—A program for analyzing time-series of satellite sensor data. *Computers & Geosciences*, *30*, 833–845.

Kimball, J. S., Running, S. W., & Nemani, R. (1997). An improved method for estimating surface humidity from daily minimum temperature. *Agricultural and Forest Meteorology*, *85*, 87–98.

Knyazikhin, Y., Martonchik, J. V., Myneni, R. B., Diner, D. J., & Running, S. W. (1998). Synergistic algorithm for estimating vegetation canopy leaf area index and fraction of absorbed photosynthetically active radiation from MODIS and MISR data. *Journal of Geophysical Research*, *103*(D24), 32257–32275.

Landsberg, J. J., & Coops, N. C. (1999). Modelling forest productivity across large areas and long periods. *Natural Resource Modelling*, *12*, 1–28.

Landsberg, J., & Sands, P. (2010). Physiological ecology of forest production. Elsevier.

Landsberg, J. J., & Waring, R. H. (1997). A generalised model of forest productivity using simplified concepts of radiation-use efficiency, carbon balance and partitioning. *Forest Ecology and Management*, *95*, 209–228.

Landsberg, J. J., Waring, R. H., & Coops, N. C. (2003). Performance of the forest productivity model 3-PG applied to a wide range of forest types. *Forest Ecology and Management*, *172*, 199–214.

Lathrop, R. G., Jr., Aber, J. D., & Bognar, J. A. (1995). Spatial variability of digital soil maps and its impact on regional ecosystem modeling. *Ecological Modelling*, *82*, 1–10.

Latta, G., Temesgen, H., Adams, D., & Barrett, T. (2010). Analysis of potential impacts of climate change on forests of the United States Pacific Northwest. *Forest Ecology and Management*, *259*, 720–729.

Lefsky, M. A. (2010). A global forest canopy height map from the moderate resolution imaging spectrometer and the geoscience laser altimeter system. *Geophysical Research Letters*, *37*, L15401.

Lefsky, M. A., Cohen, W. B., Parker, G. G., & Harding, D. J. (2002). Lidar remote sensing for ecosystem studies. *BioScience*, *52*, 19–30.

Little, E. L. Jr (1971). Atlas of United States trees, conifers and important hardwoods: Volume 1. *United States Department of Agriculture. Miscellaneous Publication* (pp. 1146).

Mäkelä, A., Landsberg, J., Alan, R., Ek, A. R., Burk, T. E., Ter-Mikaelian, M., et al. (2000). Process-based models for forest ecosystem management: Current state of the art and challenges for practical implementation. *Tree Physiology*, *20*, 289–298.

McLaughlin, S. P. (1986). Floristic analysis of the southwestern United States. *Western North American Naturalist*, *46*, 46–65.

Mulder, V. L., de Bruin, S., Schaepman, M. E., & Mayr, T. R. (2011). The use of remote sensing in soil and terrain mapping — A review. *Geoderma*, *162*, 1–19.

Myneni, R. B., Hoffman, S., Knyazikhin, Y., Privette, J. L., Glassy, J., Tian, Y., et al. (2002). Global products of vegetation leaf area and fraction absorbed PAR from year one of MODIS data. *Remote Sensing of Environment*, *83*, 214–231.

Nightingale, J. M., Fan, W., Coops, N. C., & Waring, R. H. (2008). Predicting tree diversity across the U.S.A. as a function of modeled gross primary production. *Ecological Applications*, *18*, 93–103.

Nightingale, J. M., Phinn, S. R., & Held, A. A. (2004). Ecosystem process models at multiple scales for mapping tropical forest productivity. *Progress in Physical Geography*, *28*, 241–269.

Oren, R., Ellsworth, D. S., Johnsen, K. H., Phillips, N., Ewers, B. E., Maier, C., et al. (2001). Soil fertility limits carbon sequestration by forest ecosystems in a CO_2-enriched atmosphere. *Nature*, *411*, 469–472.

Peng, C., Liu, J., Dang, Q., Apps, M. J., & Jiang, H. (2002). TRIPLEX: A generic hybrid model for predicting forest growth and carbon and nitrogen dynamics. *Ecological Modelling*, *153*, 109–130.

Peterman, W., Waring, R. H., Seager, T., & Pollock, W. L. (2012). Soil properties affect pinyon pine–juniper response to drought. *Ecohydrology*. http://dx.doi.org/10.1002/eco.1284 (published on line).

Plaut, J. A., Yepez, E. A., Hill, J., Pangle, R., Sperry, J. S., Pockman, W., et al. (2012). Hydraulic limits preceding mortality in a piñon pine–juniper woodland under experimental drought. *Plant, Cell & Environment*. http://dx.doi.org/10.1111/j.1365-3040.2012.02512.x (published on line).

Running, S. W., Waring, R. H., & Rydell, R. A. (1975). Physiological control of water flux in conifers: A computer simulation model. *Oecologia*, *18*, 1–16.

Runyon, J., Waring, R. H., Goward, S. N., & Welles, J. W. (1994). Environmental limits on net primary production and light-use efficiency across the Oregon transect. *Ecological Applications*, *4*, 226–237.

Ryan, M. G., Hubbard, R. M., Pongracic, S., Raison, R. J., & McMurtrie, R. E. (1996). Foliage, fine-root, woody-tissue and stand respiration in *Pinus radiata* in relation to nitrogen status. *Tree Physiology*, *16*, 333–344.

Schulman, E. (1954). Longevity under adversity in conifers. *Science*, *119*, 396–399.

Stape, J. L., Ryan, M. G., & Binkley, D. (2004). Testing the utility of the 3-PG model for growth of *Eucalyptus grandis*×*urophylla* with natural and manipulated supplies of water and nutrients. *Forest Ecology and Management*, *193*, 219–234.

Swenson, J. J., Waring, R. H., Fan, W., & Coops, N. (2005). Predicting site index with a physiologically based growth model across Oregon, USA. *Canadian Journal of Forest Research*, *35*, 1697–1707.

Talhelm, A. F., Pregitzer, K. S., Burton, A. J., & Zak, D. R. (2012). Air pollution and changing biogeochemistry of northern forests. *Frontiers in Ecology and the Environment*, *10*, 181–185.

Tollefson, J. (2009). Satellites beam in biomass. *Nature*, *462*, 834–835.

Tucker, C. J. (1979). Red and photographic infrared linear combinations for monitoring vegetation. *Remote Sensing of Environment*, *8*, 127–150.

Verstraete, M. M., Pinty, B., & Myneni, R. B. (1996). Potential and limitations of information extraction on the terrestrial biosphere from satellite remote sensing. *Remote Sensing of Environment*, *58*, 201–214.

Waring, R. H. (1983). Estimating forest growth and efficiency in relation to canopy leaf area. *Advances in Ecological Research*, *13*, 326–354.

Waring, R. H. (2000). A process model analysis of environmental limitations on growth of Sitka spruce plantations in Great Britain. *Forestry*, *73*, 65–79.

Waring, R. H., & Cleary, B. D. (1967). Plant moisture stress: Evaluation by pressure bomb. *Science*, *155*, 1248–1254.

Waring, R. H., Coops, N. C., Fan, W., & Nightingale, J. M. (2006). MODIS enhanced vegetation index predicts tree species richness across forested ecoregions in the contiguous U.S.A. *Remote Sensing of Environment*, *103*, 218–226.

Waring, R. H., & Franklin, J. F. (1979). Evergreen coniferous forests of the Pacific Northwest. *Science*, *204*, 1380–1386.

Waring, R. H., & Major, J. (1964). Some vegetation of the California coastal redwood region in relation to gradients of moisture, nutrients, light, and temperature. *Ecological Monographs*, *34*, 167–215.

Waring, R. H., & McDowell, N. (2002). Use of a physiological process model with forestry yield tables to set limits on annual carbon balances. *Tree Physiology*, *22*, 179–188.

Waring, R. H., Milner, K. S., Jolly, W. M., Phillips, L., & McWethy, D. (2005). A basis for predicting site index and maximum growth potential across the Pacific and Inland Northwest U.S.A. with a MODIS satellite-derived vegetation index. *Forest Ecology and Management*, *228*, 285–291.

Waring, R., Nordmeyer, A., Whitehead, D., Hunt, J., Newton, M., Thomas, C., et al. (2008). Why is the productivity of Douglas-fir higher in New Zealand than in the Pacific Northwest, USA? *Forest Ecology and Management*, *255*, 4040–4046.

Waring, R. H., & Youngberg, C. T. (1972). Evaluating forest sites for potential growth response of trees to fertilizer. *Northwest Science*, *46*, 67–75.

Weiss, M., Baret, F., Garrigues, S., & Lacaze, R. (2007). LAI and fAPAR CYCLOPES global products derived from VEGETATION. Part 2: Validation and comparison with MODIS collection 4 products. *Remote Sensing of Environment*, *110*, 317–331.

Whittaker, R. H. (1961). Vegetation history of the Pacific Coast States and the "central" significance of the Klamath region. *Madrono*, *16*, 5–23.

Yuan, H., Dai, Y., Xiao, Z., Ji, D., & Shangguan, W. (2011). Reprocessing the MODIS Leaf Area Index products for land surface and climate modelling. *Remote Sensing of Environment*, *115*, 1171–1187.

Zhang, X., Friedl, M. A., Schaaf, C. B., Strahler, A. H., Hodges, J. C. F., Gao, F., et al. (2003). Monitoring vegetation phenology using MODIS. *Remote Sensing of Environment*, *84*, 471–475.

Zheng, D., Hunt, E. R., Jr., & Running, S. W. (1996). Comparison of available soil water capacity estimated from topography and soil series information. *Landscape Ecology*, *11*, 3–14.

Zheng, G., & Moskal, M. (2009). Retrieving Leaf Area Index (LAI) using remote sensing: Theories, methods and sensors. *Sensors*, *9*, 2719–2745. http://dx.doi.org/10.3390/s90402719.

Zinke, P. J., & Strangenberger, A. G. (2000). Elemental storage in forest soils for local to global scales. *Forest Ecology and Management*, *138*, 159–165.